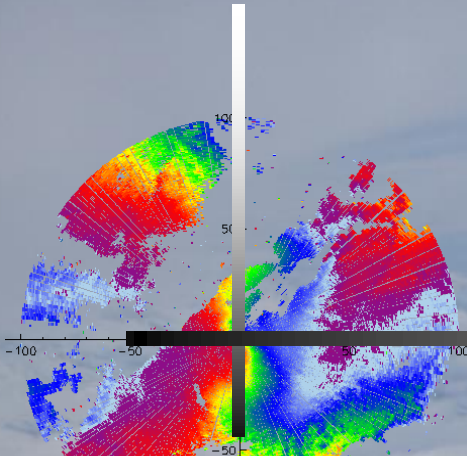


Heuristic and Quantitative Modelling of Polarimetric and temporal Properties of Weather Radar Signals from Rain and Wind-Parks



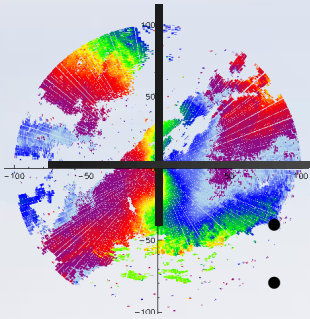
Madhu Chandra¹, Frank Gekat²

¹ Dept. of Microwave Engineering and EM Theory, Technische Universität Chemnitz, Chemnitz, Germany, madhu.chandra@etit.tu-chemnitz.de

² Selex ES GmbH, Neuss, Germany,

F.Gekat@selex-es-gmbh.com

With contributions from M.Sc. Andre Schleicher and M.Sc. Animesh Bhagwat

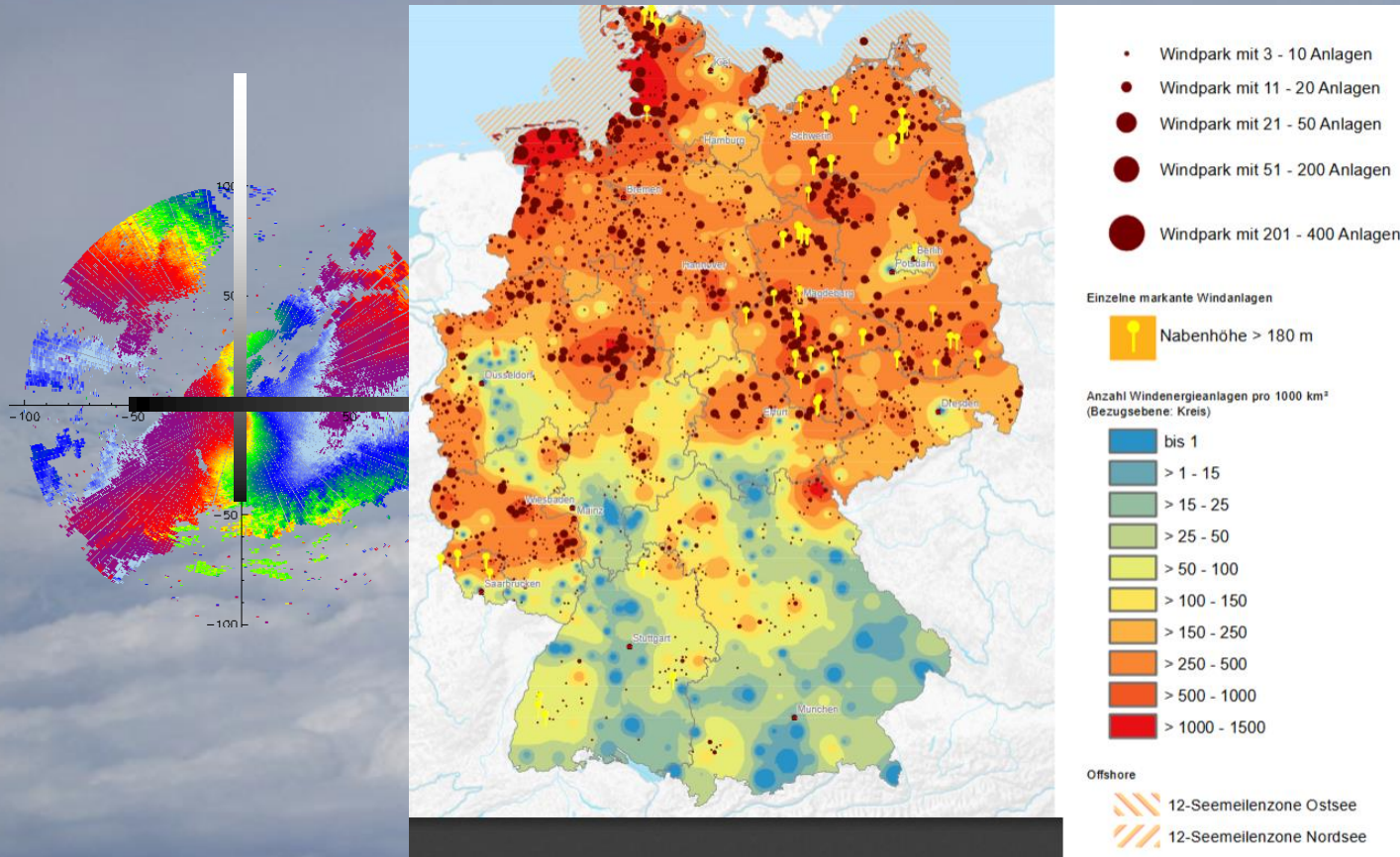


Contents

- Motivation: Wind-Parks and Weather radar Measurements
- Heuristic and Quantitative Assessment
- Basic pulsed radar measuring scheme
- Generalization of polarimetric echoes
- Generalisation of Average Complex correlations between polarimetric echoes
- Classification of Weather radar targets on the basis of their decorrelation times
- Estimating averaged backscatterd radar power from different but competing targets
- Estimating rain power and Clutter Power

**Professur für Hochfrequenztechnik und
Theoretische Elektrotechnik EMWT 2019
Toulouse**

Distribution of Windparks in Germany



Source:

https://www.bfn.de/fileadmin/BfN/daten_fakten/Dokumente/II_4_3_21_Verteilung_Elektrizitaetsgew_Wind.pdf



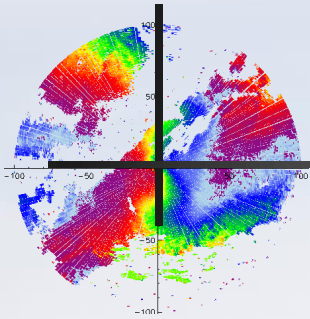
Grundparameter eines polarimetrischen Radars

- **H- und V- Polarisation**
- **Betriebsfrequenz: 5.504 GHz (C-Band)**
- **Elevation und Azimut Winkel der Antenne kontinuierlich einstellbar**
- **Maximum Reichweite: 200 KM**
- **Empfindlichkeit: -100dBm**



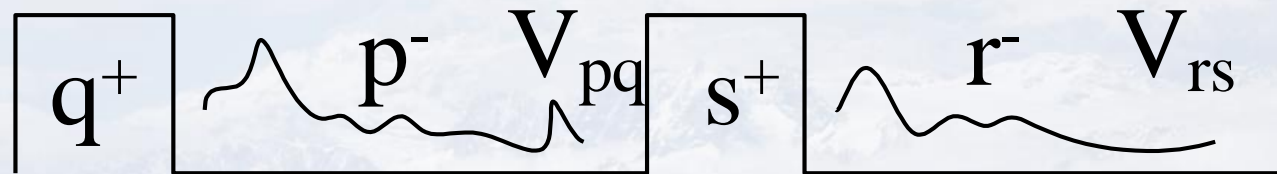
DLR, Oberpfaffenhofen





Reminder on the Pulsed Radar Method

A Generalized polarimetric notation for describing a pulse-pair-transmit-receive-measurement-cycle.



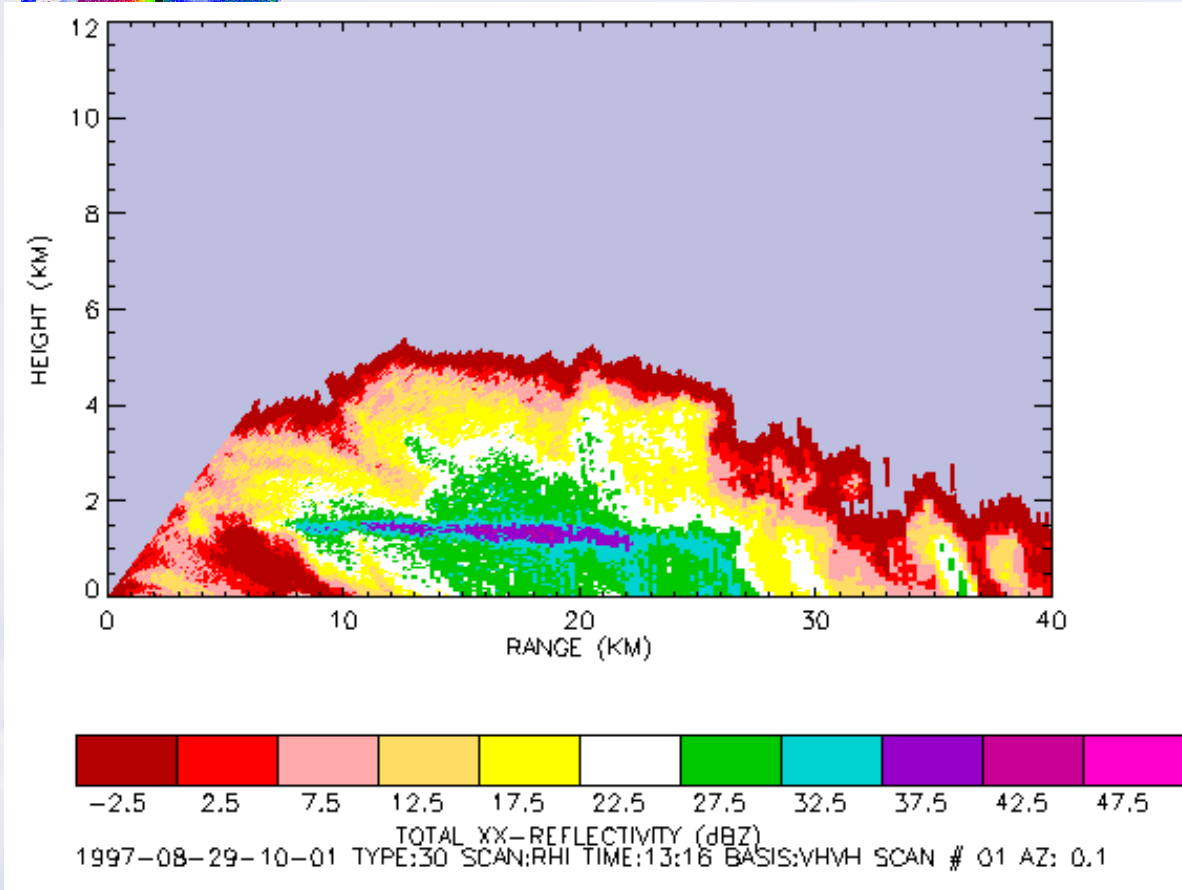
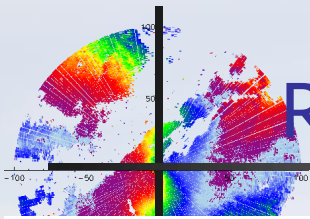
$$V_{pq} = I_{pq} + jQ_{pq}$$

$$V_{rs} = I_{rs} + jQ_{rs}$$

V_{pq} = voltage signal received with set transmit polarization q^+ and set receive polarisation p^- . The plus and minus superscripts are meant to indicate the antiparallel propagation directions

**Professur für Hochfrequenztechnik und
Theoretische Elektrotechnik EMWT 2019
Toulouse**

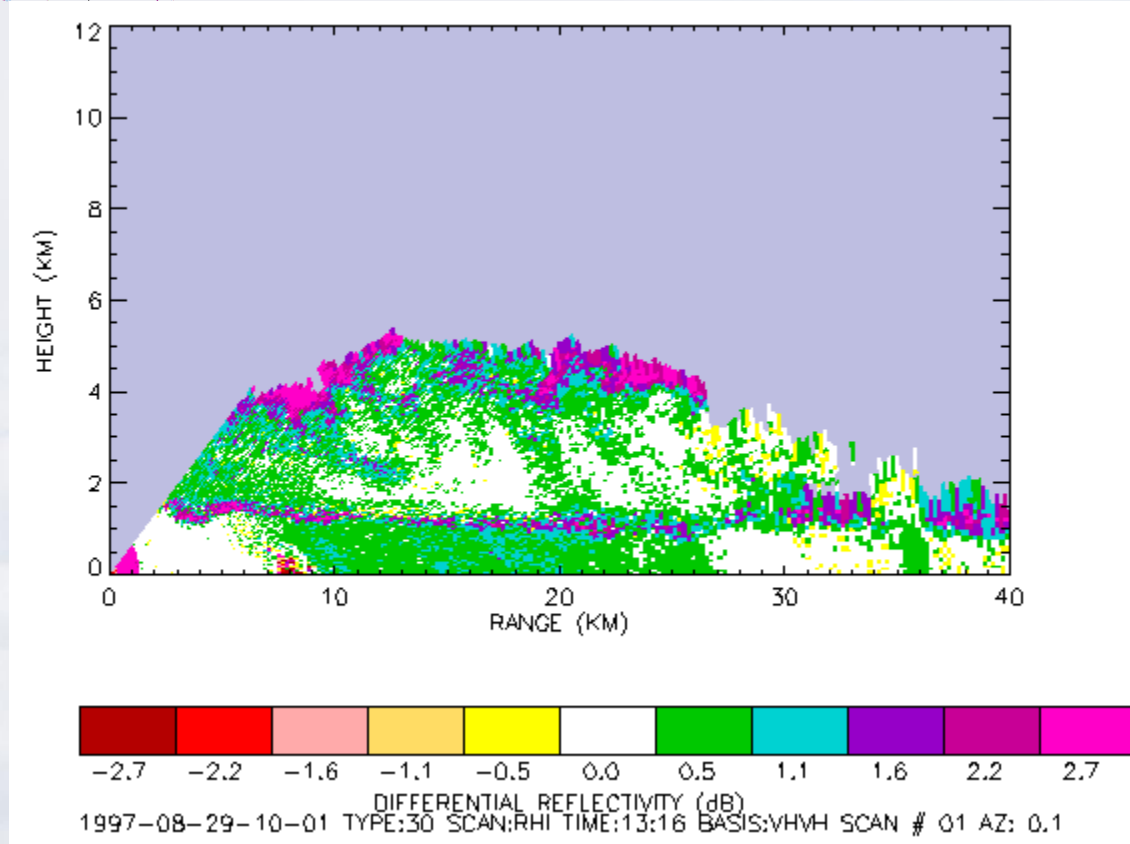
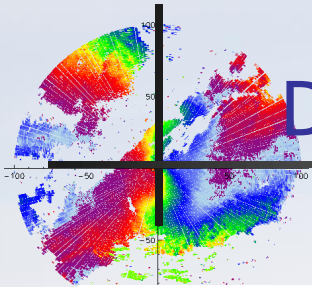
RHI-Schnitt: Range-Height Scan von $20 \log \langle |\lambda_{HH}| \rangle$



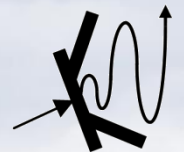
$$[S]_{H,V} = \begin{bmatrix} \lambda_{HH} & 0 \\ 0 & \lambda_{VV} \end{bmatrix}_{H,V}$$



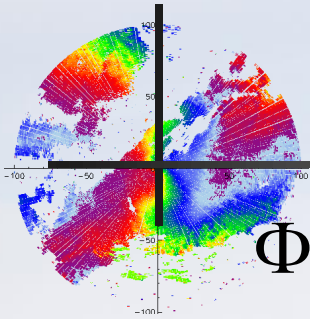
Differentielle Reflektivität



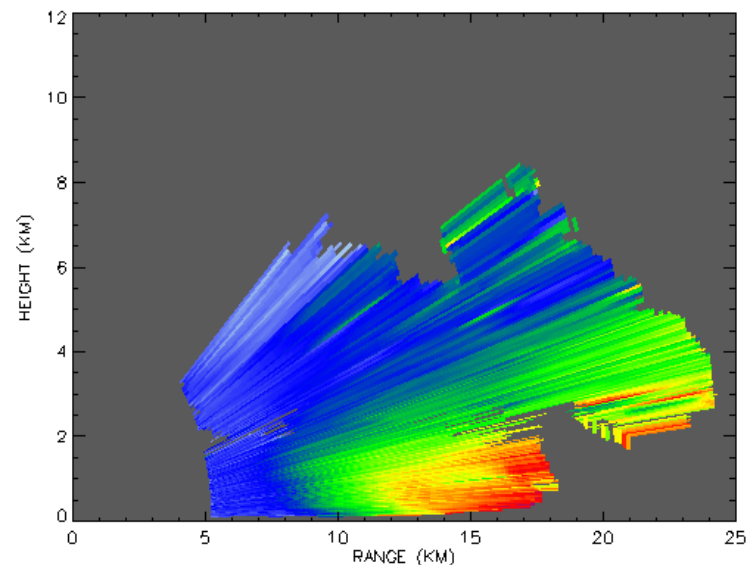
$$Z_{dr} = 10 \log \frac{\langle |S_{hh}|^2 \rangle}{\langle |S_{vv}|^2 \rangle} [dB]$$



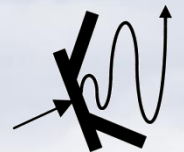
Differentielle Ausbreitungsphasen

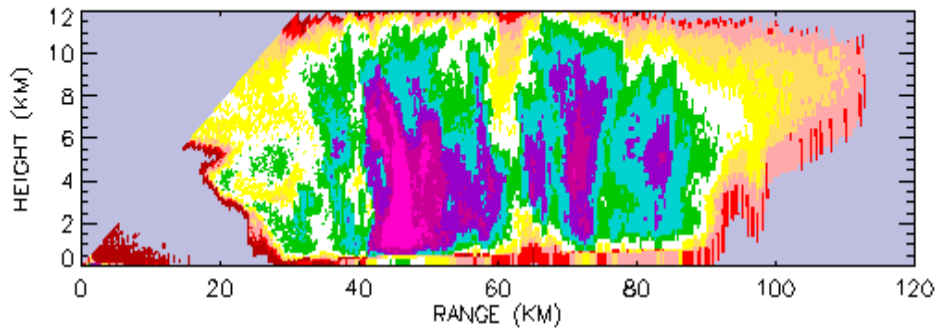


$$\Phi_{DP} = \text{Arg} \left[S_{VV}(R) S_{HH}^*(R) \right] = \text{Arg} \left[\lambda_{VV}(R) \lambda_{HH}^*(R) \right]$$

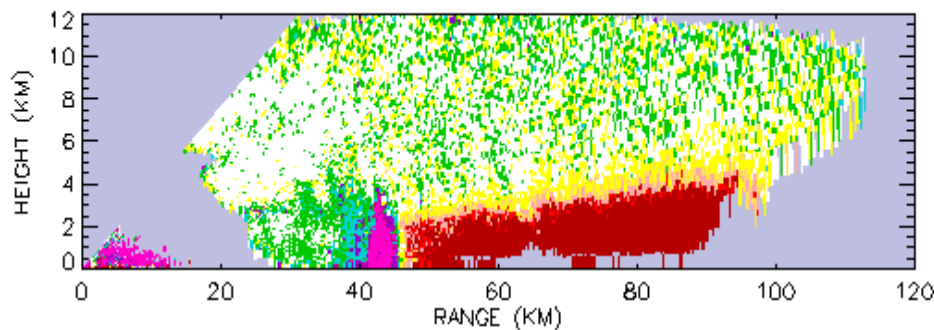


DIFF PROP PHASE YY_P_3 (DEG)
1997-06-17-10-01 TYPE:30 SCAN:RHI TIME:17:08 BASIS:VHVH SCAN # 02 AZ: 181.0





TOTAL XX-REFLECTIVITY (dBZ)
1996-06-10-05-07 TYPE:24 SCAN:RHI TIME:19:36 BASIS:VHVH SCAN # 21 AZ: 182.0



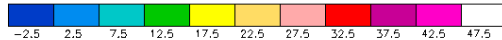
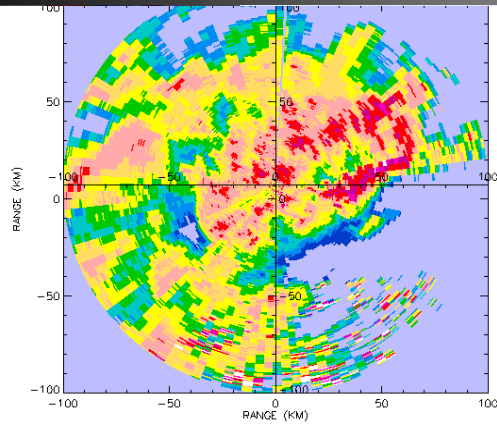
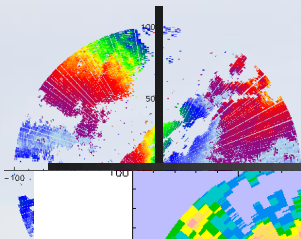
DIFFERENTIAL REFLECTIVITY (dB)
1996-06-10-05-07 TYPE:24 SCAN:RHI TIME:19:36 BASIS:VHVH SCAN # 21 AZ: 182.0

Weather Radar Measurements

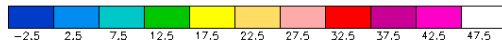
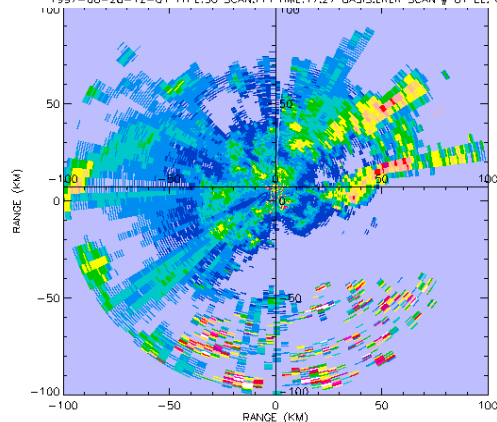


in
Zusammenarbeit
mit der DLR

Ground-Clutter Suppression using Polarisation



TOTAL XY-REFLECTIVITY (dBZ)
1997-08-28-12-01 TYPE:30 SCAN#PI TIME:17:29 BASIS:LR SCAN # 01 EL: 0.9



TOTAL XY-REFLECTIVITY (dBZ)
1997-08-28-12-01 TYPE:30 SCAN#PI TIME:17:29 BASIS:LR SCAN # 01 EL: 0.9

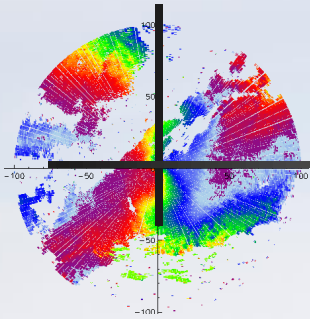
$$[S]_{LR}^{Alpen}{}_{H,V} = \begin{bmatrix} S_{LL} & S_{RL} \\ S_{RL} & S_{RR} \end{bmatrix}_{L,R}$$

$$[S]_{L,R}^{Wetter} = \begin{bmatrix} 0 & \lambda_{RL} \\ \lambda_{LR} & 0 \end{bmatrix}_{L,R}$$

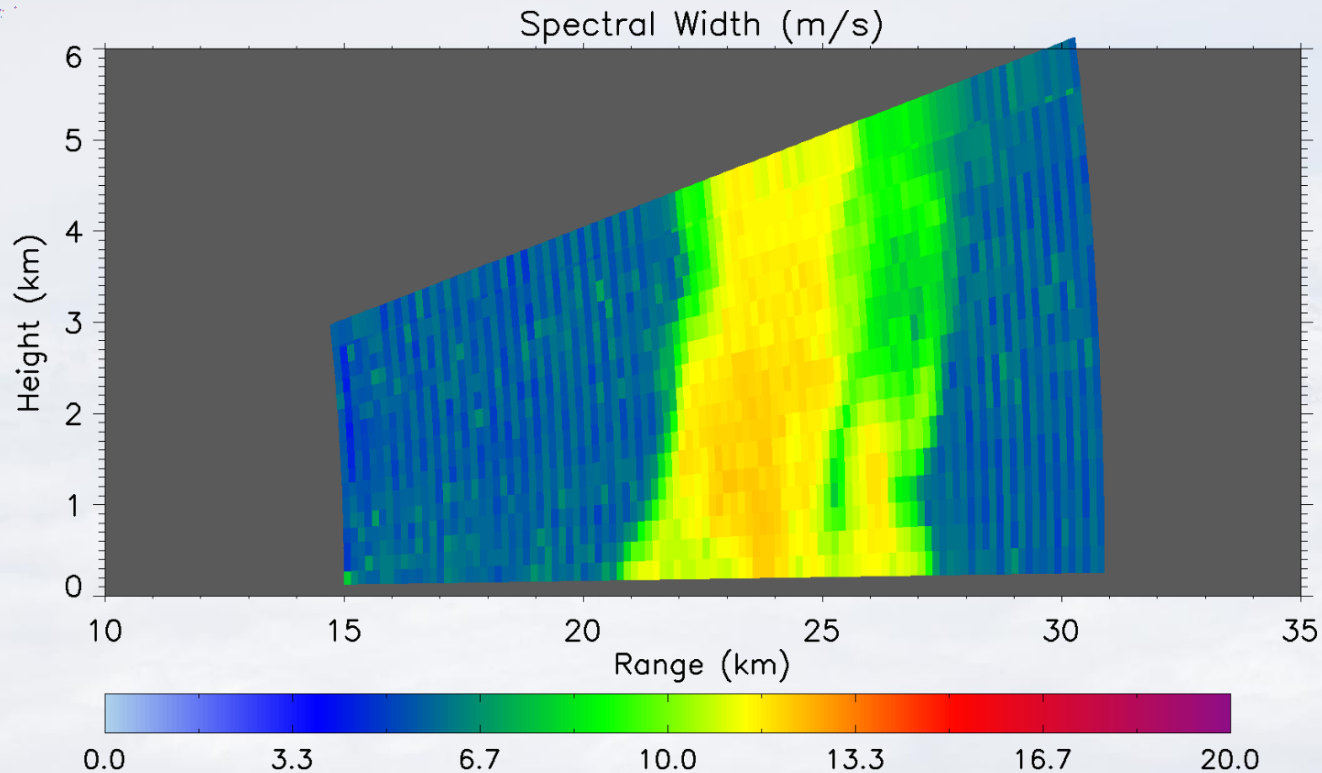
Polarimetric Measurements offer more than 10 dB of *additional* Clutter/Target discrimination

Professur für Hochfrequenztechnik und Theoretische Elektrotechnik
GEMT 2019 Toulouse



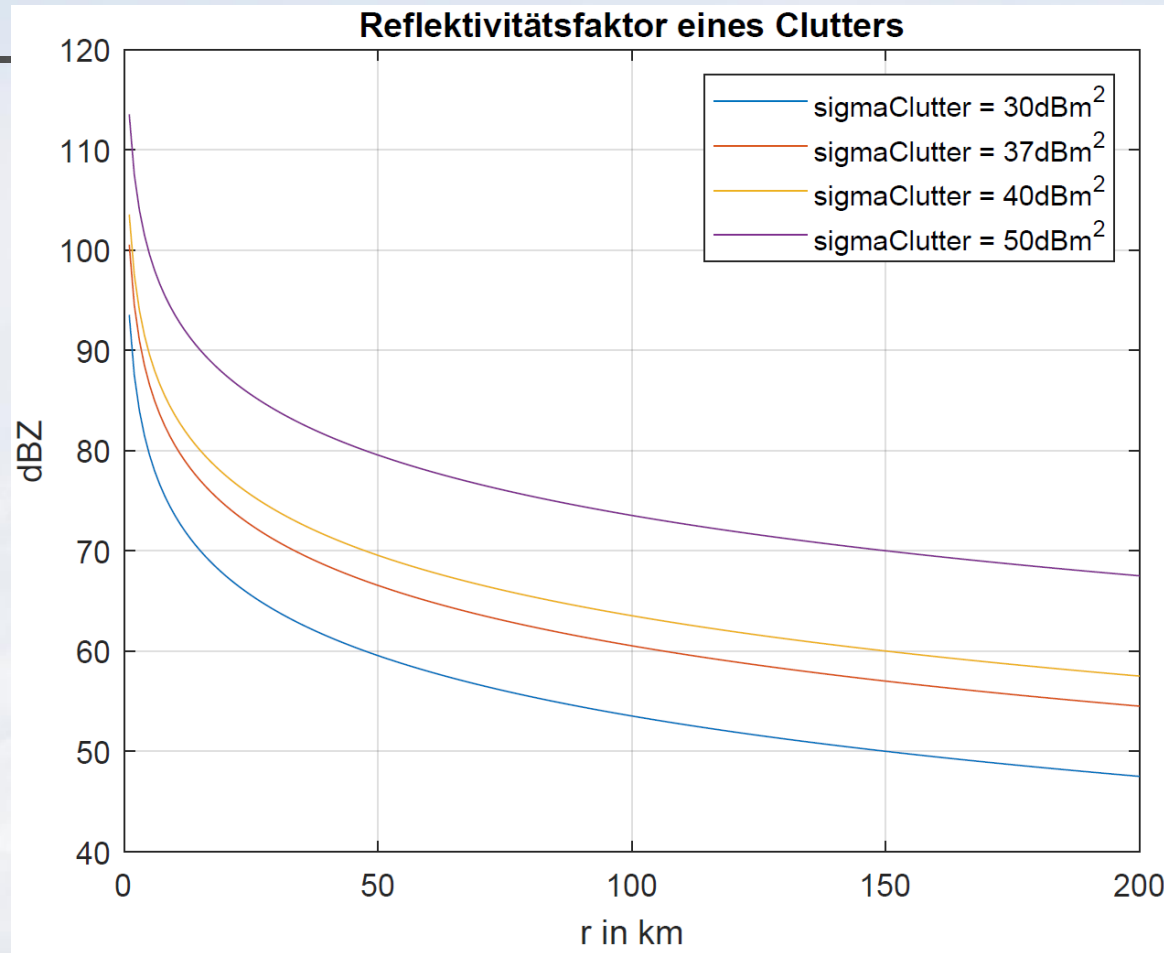
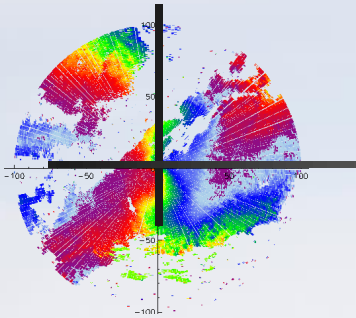


Beispiel: Doppler Spektralbreite (m/s)



	38 25 25 [<0...38]	90 90 90	0 45 90	3	IPO	D=70m, H=65m, d=6,1m (Enercon E70) Rotor in A-Stellung (0°)	[11]
45 38 43 [<0...48]	45 35 43 [3...48]	90 90 90	0 45 90	5	HF + RT, alles aus PEC	D=80m, H=60m, d=3,5m, w=3,6m Rotor in A-Stellung (0°)	[12]
45 37 47 [<0...48]	45 35 47 [<0...48]	90 90 90	0 45 90	2,4			
38 20 38 [2...57]		90 90 90	0 45 90	3	PO	D=90m, H=80m, w=3,5m (Vestas V90-3MW) Rotor in A-Stellung (0°)	[13]
45 32 35 [<0...50]	45 32 34 [<0...49]	90 90 90	0 45 90	3?	GO (SBR) + PO + PTD	D=96m, H=150m	[14]
-26 -33 -34 [-49...-26]		90 90 90	0 45 90	10,5	PO	Skaliertes Modell: D=0,7m, H=1,2m Rotorblätter aus CFK	[15]
-25 -38 -38 [-50...-25]		90 90 90	0 45 90	10,5	Labormessung		
Messwerte normalverteilt: Mittelwert: 24,7 Standardabweichung: 3,2				5,64	Realmessung mit Oktokopter	D=150m, H=140m, Entfernung: 1,7km	[16]

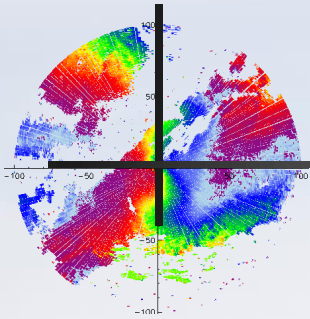
Clutter Reflectivity



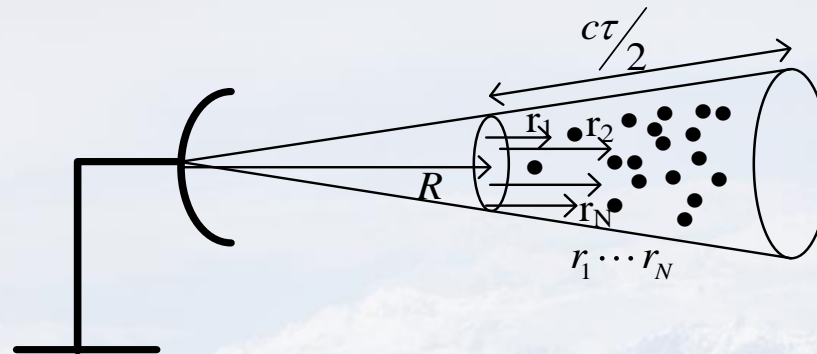
The Radarparameters used were taken from SELEX 700C Weather Radar

Θ_H	1°
λ	0,0525m
τ	0,5 μ s
c	$2,9971 \cdot 10^8 \frac{m}{s}$
$ K_m ^2$	0,92

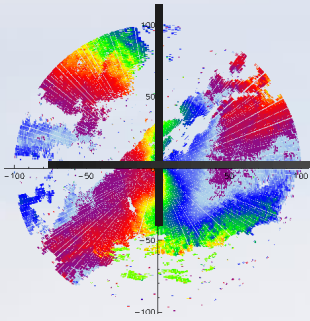
**Professur für Hochfrequenztechnik und
Theoretische Elektrotechnik EMWT 2019
Toulouse**



Pulse volume of a Weather Target



Depiction of the active pulse volume filled with hydrometeors that contribute to the instantaneous scattering amplitude of the active pulse volume. The individual scatterers are in random motion, resulting in time varying r_n 's. In scenarios with wind-park interference, sections of the wind-park structures intercept such pulse-volumes, thereby superimposing 'wind-park clutter or interference' on the weather echoes.



Physical Interpretation of the Voltage Echoes

$$V_{pq}(t) = |V_{pq}|(t)e^{j\theta_{pq}(t)} = I_{pq}(t) + jQ_{pq}(t)$$

$$= 2 \cdot \sqrt{R_A P_q^+} \frac{G\lambda}{(4\pi)^{3/2} R^2} |S_{pq}(t)| e^{j\phi_{pq}(t)} e^{-(\alpha_p + \alpha_q)R} e^{-j(\beta_p + \beta_q)R} \quad (1)$$

Where:

R_A : is the total antenna resistance (= radiation + ohmic-loss);

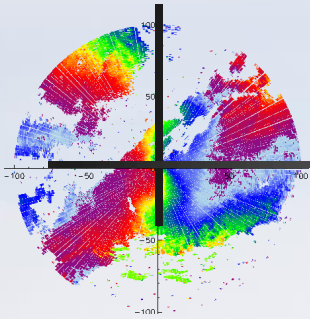
P_q^+ : is the transmit power along polarization q;

G_q : is the antenna gain

α and β : are, respectively, the effective specific attenuation and phase constants along the range R;

$\gamma = \alpha + j\beta$: is the effective complex propagation-constant outside the pulse-volume.

$S_{pq}(t)$: is the ***instantaneous effective polarimetric complex radar back-scattering amplitude***



Modelling and Classification of Weather Radar Targets

We identify and classify the following three weather radar targets according to their decorrelation times:

Weather targets (i.e. rain) of decorrelation time, τ_w .

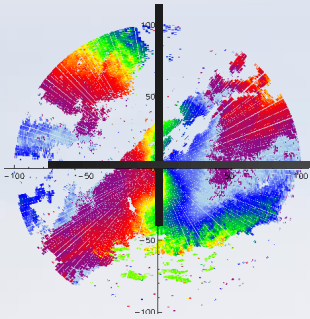
Moving Clutter (i.e. Wind parks with rotating turbines, vehicles etc.) of decorrelation time, τ_m .

Fixed Clutter (i.e. Wind parks with stationary turbines, ground clutter etc.) of decorrelation time, τ_f .

We stipulate: $\tau_w < \tau_m < \tau_f$; A key assumption!

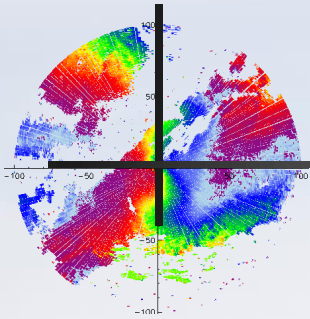
**Professur für Hochfrequenztechnik und
Theoretische Elektrotechnik EMWT 2019
Toulouse**

The Instantaneous Scattering Amplitude of a Radar Echo from a Pulse-Volume



$$S_{pq}(t) = \left(\sum_{n=1}^N \left(S_{pq}^w \right)_n e^{-\gamma_{pq} r_n(t)} \right)$$

Where, $(S_{pq}^w)_n$ is the complex instantaneous backscattering-amplitude of the n^{th} weather scatterer (for instance a raindrop) within the pulse volume shown in the previous figure, and γ_{pq} is the effective two-way complex propagation constant within the pulse volume.



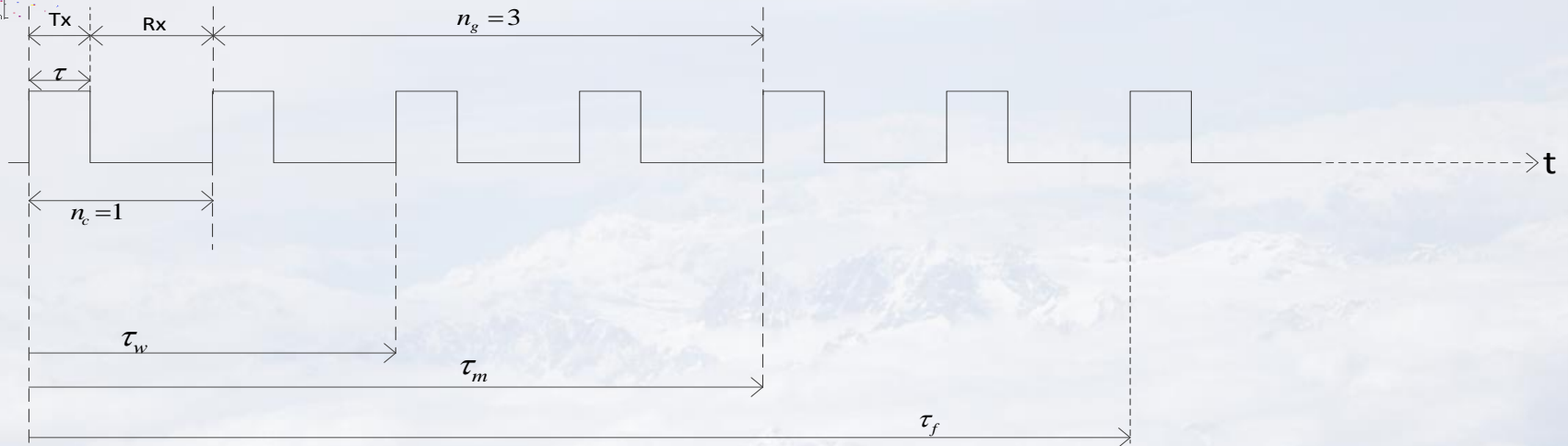
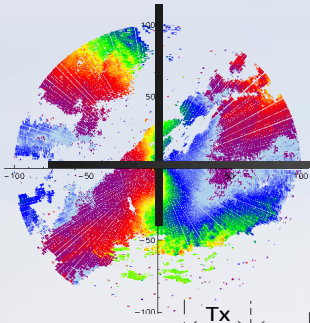
Modelling the Time Dependence of Echoes in Presence of „Clutter“

For a given pulse volume, containing all three types of scatterers, *the time dependence* of the effective polarimetric complex radar back-scattering amplitude, S_{pq} , of the active radar pulse volume, may be modelled as:

$$S_{pq}(t) = I_{pq}(t) + jQ_{pq}(t) = e^{-(\tau_w/t)} \left(\sum_{n_w=1}^{N_w} (S_{pq}^w)_{n_w} e^{-\gamma_{pq} r_{n_w}(t)} \right) + e^{-(\tau_m/t)} \left(\sum_{n_m=1}^{N_m} (S_{pq}^m)_{n_m} e^{-\gamma_{pq} r_{n_m}(t)} \right) + e^{-(\tau_f/t)} \left(\sum_{n_f=1}^{N_f} (S_{pq}^f)_{n_f} e^{-\gamma_{pq} r_{n_f}(t)} \right)$$

**Professur für Hochfrequenztechnik und
Theoretische Elektrotechnik EMWT 2019
Toulouse**

Pulse-Train-Timing Diagram for computing the complex correlations used in the proposed Methodology



The figure shows an illustrative case of the pulse-pair parameters used in the presentation: $T \cdot n_c$ (correlation delay) = $1T$ and $T \cdot n_g$ (time gap between pulse-pair-products) = $3T$. We depict the case in which the correlation delay $n_c T$ is less than τ_w whereas time gap $n_g T$ between successive products is greater than τ_w .

**Professur für Hochfrequenztechnik und
Theoretische Elektrotechnik EMWT 2019
Toulouse**

Generalised Description of Products between Complex Echoes from a Pulse-Volume

Average Complex Echo Power
(within a constant) =

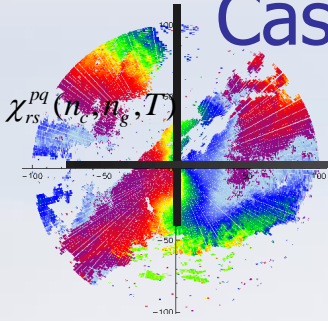
$$\chi_{rs}^{pq}(n_c, n_g) = \langle V_{pq}^*(t) \cdot V_{rs}(t + n_c T) \rangle_{n_c}^{n_g} =$$

$$\frac{1}{N_{ss}} \sum_{n=1}^{N_{ss} = N_T / (n_c + n_g)} V_{pq}^*[t_d + (n-1)(n_g + 1)T] \times \dots \times$$

$$V_{rs}[t_d + ((n-1)(n_g + 1) + n_c)T]$$

In this equation, N_{ss} is the total number of pulse-pair products over which the average value is computed, t_d is time delay of the voltage echo, T is the pulse repeat interval ($= 1/\text{PRF}$), $T \cdot n_c$ is the 'correlation lag' between the pulses paired in the products, $T \cdot n_g$ is the time gap between the successive pulse-pair products in the summation above. The possible integer values of these delay parameters are: 0, 1, 2, ...



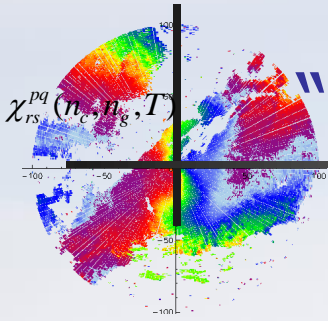


Case 1: Backscattered Power from rain and Clutter

Case 1 (All inclusive case): $n_c T \leq \tau_w$ and $\tau_w \leq n_g T < \tau_m$ and τ_f

In this case, the time-averaged pulse-pair product:

$\chi_{rs}^{pq}(n_c, n_g, T)$ for brevity called P_1 , will be proportional to backscattering from rain and all clutter targets.



Case 2: Backscattered Power from "fixed" and "moving" Clutter only (i.e. No rain)

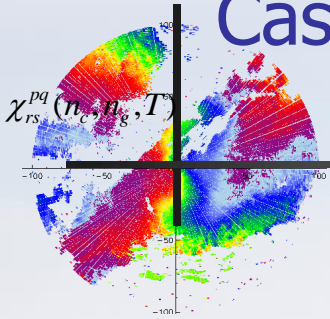
Case 2 (fixed and moving Clutter only):

$$\tau_w \ll n_c T \ll \tau_f \text{ and } \tau_m; n_g = 0$$

In this case, the time-averaged pulse-pair product:

$\chi_{rs}^{pq}(n_c, n_g, T)$ for brevity called P_2 , will be proportional to backscattering from all clutter targets (no rain present).

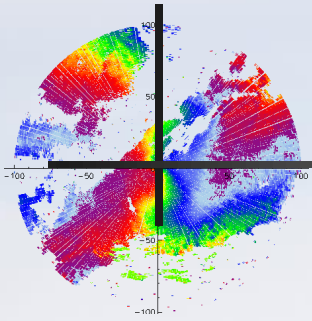
Case 3: Backscattered Power from "fixed" Clutter



Case 3 (Fixed Clutter only): $\tau_m \ll n_c T \ll \tau_f$ and $n_g = 0$

In this case, the time-averaged pulse-pair product:

$\chi_{rs}^{pq}(n_c, n_g, T)$ for brevity called P_3 , will be primarily proportional to backscattering from 'fixed' clutter.



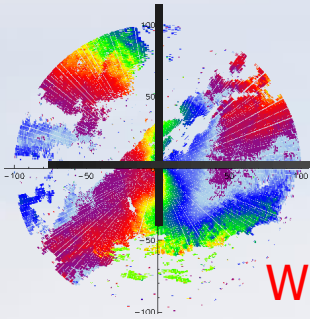
Estimating „Clutter-free“ rain power

$$P_W = P_1 - P_2$$



$$\text{Power}_{\text{weather (i.e. rain)}} = \text{Power}_{\text{rain+moving and fixed clutter}} - \text{Power}_{\text{moving and fixed clutter}}$$

Key Scattering properties-1: Doppler vs Polarisation vs Temporal variation



Polarisation.

Wind-Parks:

- Low Differential Reflectivities and linear Depolarisation ratio (LDR)
- Abrupt and Large Differential propagation phase (an educated guess)

Rain:

- Modest Differential Reflectivities (ZDR) and linear Depolarisation ratio $LDR = [10 \log(\frac{Z_{VH}}{Z_{HH}})]$
- Monotonically increasing Differential propagation phase (an educated guess)

Doppler.

Wind-Parks:

- Potentially large spectral widths

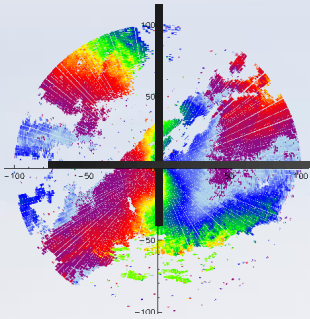
Rain:

- Modest spectral widths

**Professur für Hochfrequenztechnik und
Theoretische Elektrotechnik EMWT 2019
Toulouse**



Key Scattering properties-2: Doppler vs Polarisation vs Temporal variation



Temporal Variation.

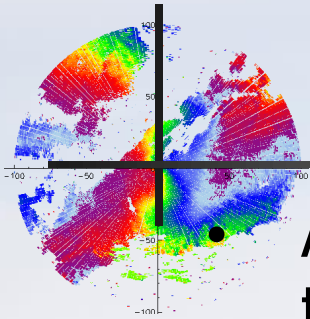
Wind-Parks:

- Slow variation over several ms

Rain:

- Rapid variations occurring a period of about 1 ms

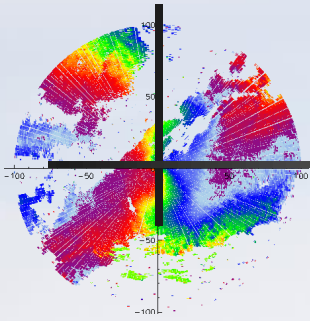
**Professur für Hochfrequenztechnik und
Theoretische Elektrotechnik EMWT 2019
Toulouse**



Conclusions-1

- A judicious choice of the correlation delay $n_c * T$ and the time gap between the pulse-pair-products, $n_g * T$, can be implemented in the calculation of the echo powers P_1 , P_2 , and P_3
- Strategy for estimating τ_w , τ_m , and τ_f :
A fairly high PRF (say typically > 3000 Hz for C-Band applications), can be used to record a large number of echoes with a slow scanning rate. This will give a high dwell-time and fine time-resolution data that can, in turn, be exploited to estimate the decorrelation times τ_w , τ_m , and τ_f .

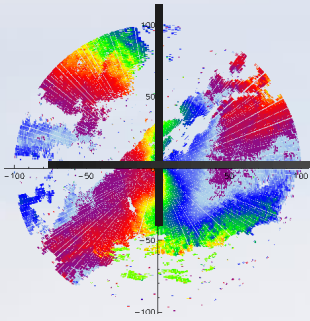
**Professur für Hochfrequenztechnik und
Theoretische Elektrotechnik EMWT 2019
Toulouse**



Conclusions-2

- Adding Polarimetric and Doppler separation in tandem should provide extra 'Signal-to-Clutter discrimination' !

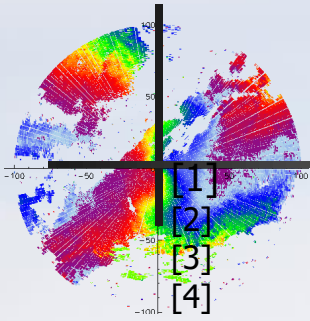
**Professur für Hochfrequenztechnik und
Theoretische Elektrotechnik EMWT 2019
Toulouse**



Outlook

- We need data to test the efficacy of the proposed Methodology!
- Potential Partners are welcome!

**Professur für Hochfrequenztechnik und
Theoretische Elektrotechnik EMWT 2019
Toulouse**



Literature used and Consulted

- [1] Fraunhofer ISE: Studie Stromgestehungskosten Erneuerbare Energien März 2018
- [2] Destatis
- [3] https://gwec.net/wp-content/uploads/vip/GWEC_PRstats2017_EN-003_FINAL.pdf
- [4] Erich Hau: Windenergieanlagen – Grundlagen, Technik, Einsatz, Wirtschaftlichkeit. 5. Auflage. Springer, Berlin/Heidelberg 2014
- [5] <https://www.iwr-institut.de/de/presse/presseinfos-energiewende/strompreise-fuer-verbraucher-steigen-boersen-strompreise-sinken-auf-rekordtiefs>
- [6] https://www.bfn.de/fileadmin/BfN/daten_fakten/Dokumente/II_4_3_21_Verteilung_Elektrizitaetsgew_Wind.pdf
- [7] <https://www.umweltbundesamt.de/themen/mindestabstaende-bei-windenergieanlagen-schaden-der>
- [8] Stromreport 2016
- [9] Sun-Hong Kim, Yong-Gwon Park, and Sung-Soo Kim, „Double-layered microwave absorbers composed of ferrite and carbon fiber composite laminates“, phys. stat. sol. (c) 4, No. 12, 4602–4605 (2007) / DOI 10.1002/pssc.200777374
- [10] Hans J. Liebe, George A. Hufford and Takeshi Manabe, „A Model for the Complex Permittivity of Water at Frequencies Below 1THz“, International Journal of Infrared and Millimeter Waves, Vol. 12, No. 7, 1991
- [11] G. Greving, W.-D. Biermann, R. Mundt, „Wind Turbines and Radar – The Radar Cross Section RCS a Useful Figure for Safeguarding?“, International Radar Symposium 2007
- [12] David Jenn and Cuong Ton, „Wind Turbine Radar Cross Section“, International Journal of Antennas and Propagation, Volume 2012, Article ID 252689, 14 pages, doi:10.1155/2012/252689
- [13] I. Suci, L. Anton, T.-C. Oroian und R.-D. Raicu, „Some aspects about wind turbines as radar targets“
- [14] F. Weinmann, „Accurate Prediction of EM Scattering by Wind Turbines“, EuCAP 2014
- [15] F. Kong, Y. Zhang, R. Palmer, Y. Bai, „Wind Turbine Radar Signature Characterization by Laboratory Measurements“
- [16] J. Bredemeyer, K. Schubert, J. Werner, T. Schrader, M. Mihalachi, „Comparison of principles for measuring the reflectivity values from wind turbines“